Nucleic Acids Research, 2006, Vol. 34, No. 6 ***e51***
doi:10.1093/nar/gkl135

A novel magnetic resonance-based method to measure gene expression in living cells

Sewon Ki[1], Fuminori Sugihara[1], Koji Kasahara[1], Hidehito Tochio[1], Azusa Okada-Marubayashi[1], Setsuko Tomita[1], Masahito Morita[1], Mitsunori Ikeguchi[1], Masahiro Shirakawa[2,3,*] and Tetsuro Kokubo[1,3,*]

[1]International Graduate School of Arts and Sciences, Yokohama City University, Yokohama 230-0045, Japan, [2]Graduate School of Engineering, Kyoto University, Kyoto 615-8510, Japan and [3]CREST, Japan Science and Technology Corporation, Saitama 332-0012, Japan

Received January 3, 2006; Revised and Accepted March 14, 2006

ABSTRACT

In unicellular and multicellular eukaryotes, elaborate gene regulatory mechanisms facilitate a broad range of biological processes from cell division to morphological differentiation. In order to fully understand the gene regulatory networks involved in these biological processes, the spatial and temporal patterns of expression of many thousands of genes will need to be determined in real time in living organisms. Currently available techniques are not sufficient to achieve this goal; however, novel methods based on magnetic resonance (MR) imaging may be particularly useful for sensitive detection of gene expression in opaque tissues. This report describes a novel reporter gene system that monitors gene expression dynamically and quantitatively, in yeast cells, by measuring the accumulation of inorganic polyphosphate (polyP) using MR spectroscopy (MRS) or MR spectroscopic imaging (MRI). Because this system is completely non-invasive and does not require exogenous substrates, it is a powerful tool for studying gene expression in multicellular organisms, as well.

INTRODUCTION

In situ hybridization is the most precise, currently available method for obtaining spatial information on gene expression at the subcellular level. However, a major drawback of this method is that it cannot be performed in living cells or in real time: the cells or tissues to be analyzed must be immobilized and exposed to harsh chemicals that are incompatible with living cells. Thus, spatial and temporal information on gene expression cannot be measured simultaneously using *in situ* hybridization technology. In recent years, several non-invasive methods for detecting gene expression have been developed, which do not have this limitation. These methods use reporter genes, such as luciferase or green fluorescent protein, whose expression stimulates an optically detectable signal (1,2). Although these methods can be used in living cells, the optical signals on which the methods depend only penetrate 1–2 cm of tissue; thus, internal tissues of animal or human subjects cannot be analyzed, because the gene expression signal is obscured by light absorption and/or light scattering before it can reach the signal detector (3). Radionuclide imaging methods such as positron emission tomography (PET) and single-photon emission tomography (SPECT) offer the advantages of a non-invasive method and can measure gene expression in internal tissues (3). These techniques are well-suited for clinical use, but the spatial resolution, which is 1–2 mm, is not sufficient for research applications that demand resolution at or below the single cell level. A second disadvantage of these methods is that they require exposure of the subject to radioactive isotopes, which could be undesirable or disallowed for some applications.

MR spectroscopic imaging (MRI) is a non-invasive method with a spatial resolution at least 10 times greater than radionuclide imaging that can be used to visualize deep tissues (3). Weissleder (4) and Meade (5) were among the first to use MRI-based detection with reporter genes encoding the transferrin receptor and β-galactosidase, respectively, to analyze gene expression in cells treated with specially designed

*To whom correspondence should be addressed at Division of Molecular and Cellular Biology, Science of Supramolecular Biology, International Graduate School of Arts and Sciences, Yokohama City University, 1-7-29, Suehiro-cho, Tsurumi-ku, Yokohama, Kanagawa 230-0045, Japan. Tel: +81 045 508 7237; Fax: +81 045 508 7369; Email: kokubo@tsurumi.yokohama-cu.ac.jp
*Correspondence may also be addressed to M. Shirakawa. Laboratory of Molecular Design, Department of Molecular Engineering, Graduate School of Engineering, Kyoto University, Kyoto-Daigaku Katsura, Nishikyo-ku, Kyoto 615-8510, Japan. Tel: +81 075 383 2535; Fax: +81 075 383 2541; Email: shirakawa@moleng.kyoto-u.ac.jp

substrates for these gene products. More recently, an MRI-based reporter system was developed using either the heavy subunit of ferritin or the light and heavy subunits of ferritin. This system does not require use of a specially designed substrate, but depends on the fact that ferritin is a metalloprotein that becomes superparamagnetic when it binds endogenous iron (6,7). This method, which was developed and applied in mice, may be more versatile than other non-invasive methods which require exogenous substrate. However, MRI contrast obtained by the ferritin system is limited, since the spin–lattice (7) or spin–spin (6,7) NMR relaxation rate of water proton magnetizations was reported to be typically enhanced only about a factor of two by the presence of the iron–ferritin complex, and thus the complex serves as a negative contrast agent in T_2- and T_2*-weighted images. The acquired MRI images may not be straight-forwardly interpreted, as the relaxation rates can be affected by other factors and may not be suitable for fully quantitative measure of gene expression.

Polyphosphate (polyP), a linear polymer of orthophosphate residues linked by high-energy phosphoanhydride bonds, is found in all organisms from bacteria to mammals (8). In yeast, most of the cellular polyP (~99%) is in the vacuole where it presumably serves as both phosphate storage and a cation chelator (8). The amount of polyP in the cell depends on the function of the vacuolar transporter chaperone (Vtc) complex (9) and the vacuolar H^+-ATPase (V-ATPase) (10). Strains defective in either complex produce almost no detectable polyP, but still grow normally on acidic YPD media (data not shown) (11). These observations indicate that polyP is dispensable for growth under normal conditions and suggest that the polyP system could be manipulated without deleterious effects in living cells.

This study describes a novel MRS/MRI-based reporter system that quantifies gene expression in living cells by measuring the accumulation of inorganic polyP. This method does not require exogenous substrate and is suitable for quantitative studies of gene expression in internal tissues. In order to characterize this method, initial studies were carried out in *Saccharomyces cerevisiae*, because yeast accumulate polyP at a higher concentration (~120 mM) than other eukaryotes (8) and because yeast cells are amenable to genetic manipulation.

MATERIALS AND METHODS

Yeast strains

Standard techniques were used for yeast growth and transformation (12). The yeast strains used in this study are listed in Supplementary Table 1. Oligonucleotide sequences used for the strain construction are listed in Supplementary Table 2. More detailed information is also available on request.

The YTK6337 strain was generated from BY4742 (EUROSCARF) by a fusion PCR-mediated gene replacement method (13) using two pairs of primers, TK3950/4012 and TK4011/3977. The strain was developed as a control strain for studies examining the function of the TATA box binding protein (TBP) associated factor 1 (TAF1). In the present study, the endogenous promoter spanning up to 100 bp upstream of the translational initiation site (A of ATG as +1) of *VTC1* of the YTK6337 strain was replaced with one of six different promoters to generate the YTK6352, 6353, 6356, 6359, 6362 and 6365 strains by a fusion PCR-based method. The PCR fragments used for each promoter replacement were amplified by two or three pairs of primers as follows (the amplified marker gene or promoter region is shown in parentheses): TK3755/3756 (*His3MX6*) + TK3757/3758 (*RPS5*, −593 to +139 bp, transcriptional initiation site is +1), TK3755/3756+TK3759/3758 (*RPS5*, −87 to +139 bp), TK3755/3756+TK3760/3762 (*RPS5*, −450 to −361 bp) + TK3761/3758 (*RPS5*, −87 to +139 bp), TK3755/3756 + TK3763/3765 (*CLN2*, −100 to +175 bp, transcriptional initiation site is +1), TK3755/3756+TK3760/3767 (*RPS5*, −450 to −361 bp)+TK3766/3765 (*CLN2*, −100 to +175 bp), and TK3755/3756+TK3768/3765 (*CLN2*, −543 to +175 bp), respectively. Similarly, the YTK6395, 6415 and 6489 strains were generated from BY4742 by a PCR-based method using primer pairs of TK3755/3756+TK4390/4391 (*GAL1*, −453 to +1 bp, translational initiation site is +1), TK4985/4986 [*His3MX6-GAL1* promoter (−541 to +1 bp)-3 × HA epitope tag] and TK4981/3756 (*His3MX6*) + TK4390/4982 (*GAL1*, −453 to +1 bp), respectively. The YTK6397 strain was generated from YTK6395 by a PCR-based method using the primer pair TK4650/4651 (3 × HA epitope tag-*ADH1* terminator-*kanMX6*).

The endogenous promoter of *VMA2* in BY4741 (EUROSCARF) was replaced with the six promoters described above to generate YTK6526, 6530, 6537, 6533, 6534 and 6527 using the following primer pairs: TK4981/3756 + TK3757/5275 (*RPS5*, −593 to +139 bp), TK4981/3756 + TK3759/5275 (*RPS5*, −87 to +139 bp), TK4981/3756 + TK3760/3762 (*RPS5*, −450 to −361 bp) + TK3761/5275 (*RPS5*, −87 to +139 bp), TK4981/3756 + TK3763/5276 (*CLN2*, −100 to +175 bp), TK4981/3756 + TK3760/3767 (*RPS5*, −450 to −361 bp) + TK3766/5276 (*CLN2*, −100 to +175 bp) and TK4981/3756 + TK3768/5276 (*CLN2*, −543 to +175 bp), respectively. The PCR templates used were pFA6a-kanMX6 (14) for TK4011/3977, pFA6a-His3MX6 (14) for TK3755/3756 and TK4981/3756, pFA6a-3HA-kanMX6 (14) for TK4650/4651, pFA6a-His3MX6-PGAL1-3HA (14) for TK4985/4986 and yeast genomic DNA for the other primers.

All gene replacements were confirmed by PCR, Southern blot and genomic DNA sequencing.

Northern blot analyses

Northern blot analyses were performed as described previously (15). To prepare the probes, DNA fragments surrounding the initiating methionine (*VMA2* and *ADH1*) or corresponding to the entire open reading frame (*VTC1*) were amplified by PCR from yeast genomic DNA, purified and ^{32}P-labeled by random priming.

Immunoblot analyses

Immunoblot analyses were conducted as described previously (16). Polyclonal antibodies directed against TBP were prepared as described (16). Antibodies against the HA epitope tag (F7, mouse monoclonal) were purchased from Santa Cruz Biotechnology, Inc. (Santa Cruz, CA).

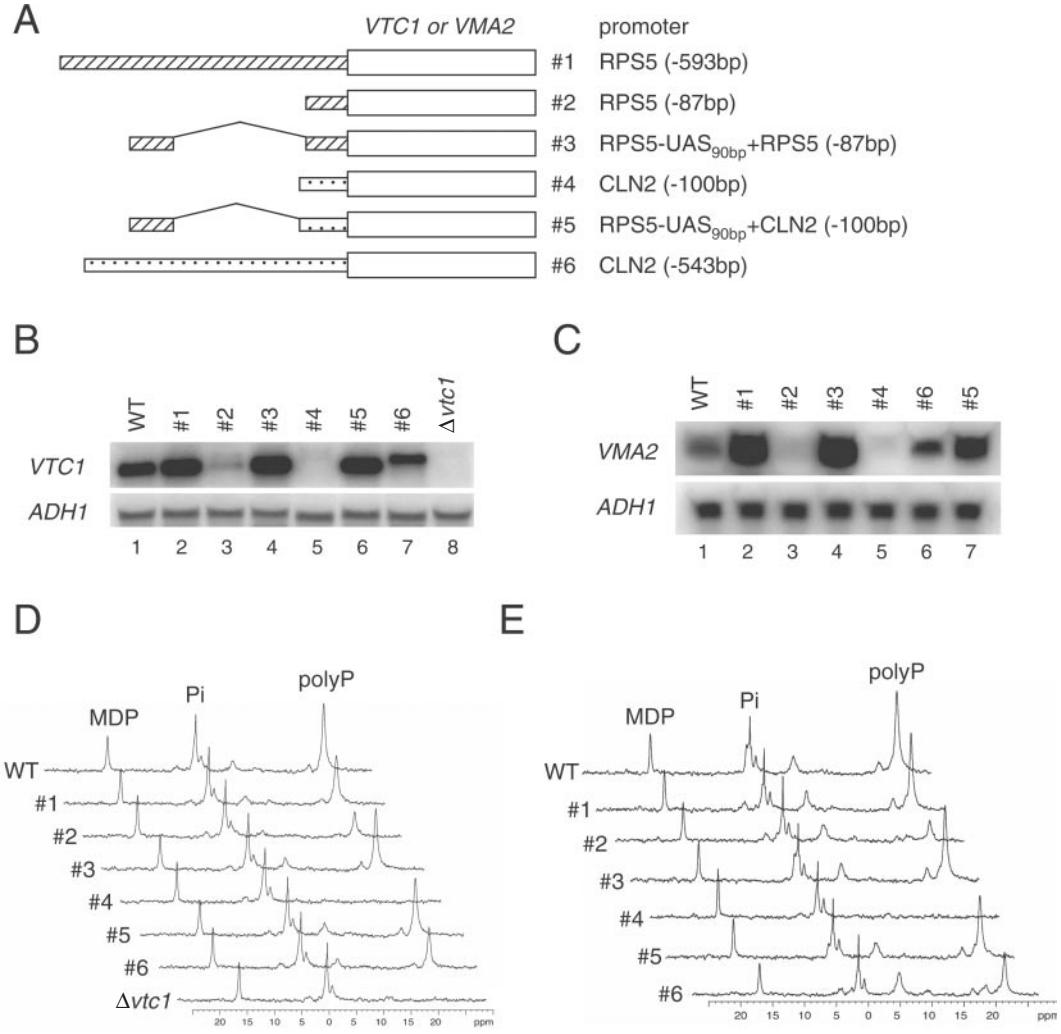

Figure 1. Transcriptional activity *VTC1* or *VMA2* under control of six different promoters. Gene activity was detected by northern blot and *in vivo* MR spectroscopy (MRS). (**A**) Schematic diagram of the reporter constructs used to express *VTC1* or *VMA2*. The sequences derived from the *RPS5* and *CLN2* promoters are shown as hatched and dotted rectangles, respectively. The regions included in each construct (#1–6) are indicated at the right. (**B**) Total RNA was extracted from cells growing logarithmically at 30°C in YPD and analyzed by northern blot using a probe for *VTC1* mRNA (upper panel). Transcription of *VTC1* was driven by the endogenous promoter (WT, lane 1) or heterologous promoters #1–6 (lanes 2–7). The Δ*vtc1* strain was used as a negative control (lane 8) to show that the gene expression signals are specific to *VTC1*. The blot was probed for *ADH1* mRNA as a control for equal loading (lower panel). (**C**) Transcription of *VMA2* and *ADH1* in the indicated strains were measured by northern blot as described for panel (B). (**D**) ^{31}P-MRS analysis of *VTC1* gene expression was performed using the same strains as in panel (B). Strain number is indicated to the left of each MRS scan. Peaks corresponding to MDP, inorganic phosphate (Pi) and inorganic polyP are marked at the top. MDP was added at a known concentration as a chemical shift standard. (**E**) ^{31}P-MRS analysis of *VMA2* expression was performed as described in (D) using the same strains as in panel (**C**). Strain number is indicated to the left of each MRS scan.

In vivo MR spectroscopy and MRI

^{31}P-NMR spectra were recorded on a DRX-500 spectrometer (Bruker, Germany) equipped with a standard bore (54 mm) 11.7 T magnet. ^{1}H-MRI and ^{31}P-MRI were recorded on the same spectrometer equipped with a Micro5 imaging probehead.

For MR spectroscopy, samples were transferred into a 5 mm NMR tube and filled with a mixture of 450 µL YPD media and 50 µL $^{2}H_2O$ (CIL, USA) containing 100 µg methylene diphosphonic acid (MDP) (Fulka, Germany), as both a concentration and chemical shift standard. The assignments of the peaks in the ^{31}P-NMR spectrum were given by reference (17). The data were acquired by applying $\pi/2$ pulses at 1 s intervals with a sweep width of 16 181 Hz. A total of 16 384 complex points were acquired. For each measurement 512 transients were accumulated. Data acquisition and analysis were performed using XWinNMR software (Bruker). The quantities of inorganic polyP were estimated by the ratio of integrated peak areas of polyP and MDP.

For MRI, samples were transferred into a 0.8 mm outer diameter capillary glass tube (Hilgenberg, Germany). The bottom of the tube was sealed with a sealing compound (Fisher, USA). The tube was then centrifuged at 1000 r.p.m. for 3 min to pellet the yeast cells. The tubes containing test samples and a positional reference (water) were put into an 8 mm NMR tube, as depicted in Figure 3A. A 3D ^{1}H image was acquired to define the positions of samples. Subsequently, the 2D image of polyP in which the polyP signal was integrated longitudinally along the axis of each capillary tube was acquired by the

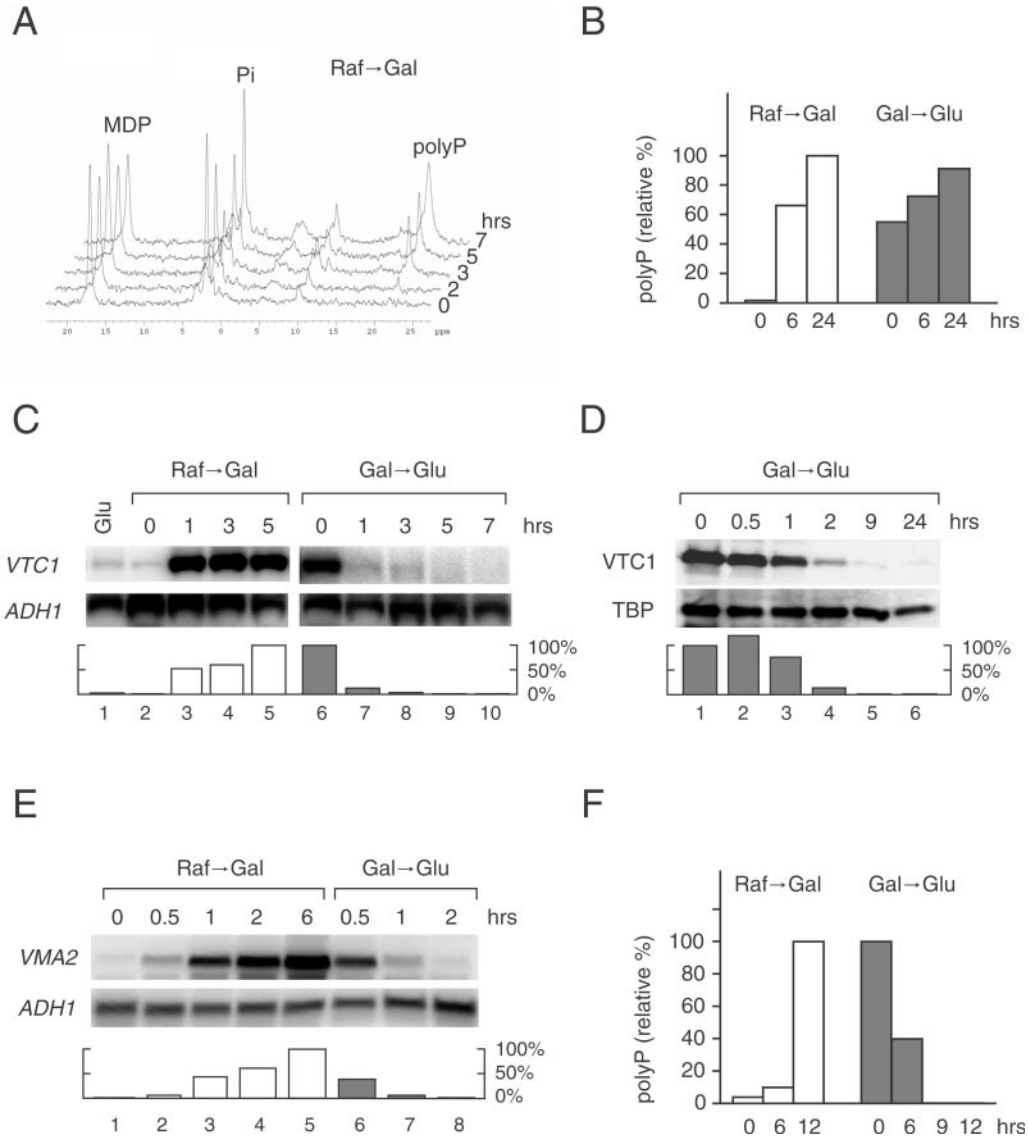

Figure 2. Kinetic analysis of expression of *VTC1* and *VMA2* reporter genes under control of the *GAL1* promoter. (**A**) Log phase yeast strains expressing *VTC1* from the *GAL1* promoter were cultured at 30°C in raffinose-containing media and shifted to galactose-containing media at $t = 0$. Samples were withdrawn at the indicated times and analyzed by ^{31}P-MRS. (**B**) Samples were prepared as described in panel (A) using cells shifted from raffinose to galactose (open bar, left) or from galactose to glucose (hatched bar, right). PolyP was measured by ^{31}P-MRS as shown in panel (A). The integral of the polyP peak was normalized to the MDP peak and the percentage of the maximum polyP signal ($t = 24$ h after the shift from raffinose to galactose) was calculated. (**C**) Samples were prepared as described in panel (B) and analyzed by northern blot with a probe for *VTC1*. The *VTC1* transcript was normalized to the *ADH1* transcript and the percentage of the maximum value for each data was calculated. (**D**) Samples were prepared as described in panel (B) and used for immunoblot analysis with antibody to HA-tagged VTC1. VTC1 protein was quantified and normalized to TATA box binding protein (TBP). Values in bar graph are the percentage of VTC1 at $t = 0$ (lane 1). Note that the strains expressing HA-tagged or untagged VTC1 protein produced almost the same amounts of polyP irrespective of endogenous or heterologous promoters. (**E**) Samples were prepared as described in panel (B) using yeast cells expressing HA-tagged *VMA2* under the control of the *GAL1* promoter. Northern blot analysis was carried out using probes for *VMA2* (upper) or *ADH1* (lower). *VMA2* transcript was normalized to *ADH1* and the percentage of maximum VMA2 expression ($t = 6$ h after the shift from raffinose to galactose) was calculated. (**F**) PolyP was quantified by ^{31}P-MRS in yeast cells expressing HA-tagged *VMA2* under the control of the *GAL1* promoter. Samples were prepared at the indicated time after media switching as described in (B). The integral of the polyP peak was normalized to the MDP peak and the percentage of the maximum polyP signal ($t = 12$ h after the shift from raffinose to galactose) was calculated.

chemical shift selective imaging method (CHESS) (18). For the CHESS, a $\pi/2$ pulse to excite ±1500 Hz region centered at the polyP signal with a Gaussian shaped and a non-selective rectangular π pulse were used. The sweep width was 5000 Hz, and TR and TE were 750 and 1.4 ms, respectively. The matrix size was 32×16 (zero-filled to 64×32 for analysis) with the field of view (FOV) of 1 cm × 1 cm. For each measurement, 256 transients were accumulated. No slice selective gradient was used. The obtained images were analyzed using ParaVision software (Bruker).

RESULTS AND DISCUSSION

Initial studies were carried out to determine whether *VTC1* and *VMA2,* which encode subunits of the Vtc complex and the

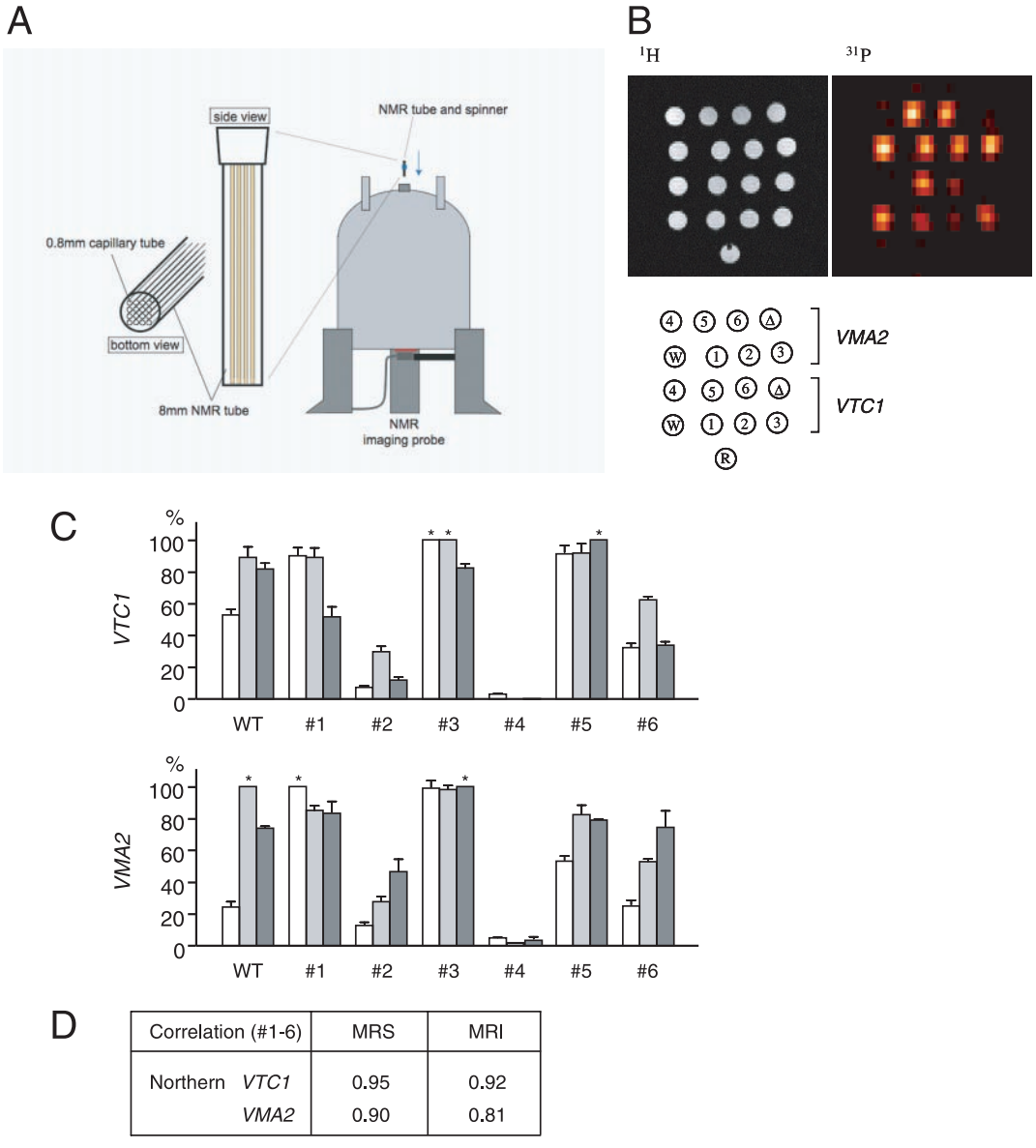

Correlation (#1-6)	MRS	MRI
Northern *VTC1*	0.95	0.92
VMA2	0.90	0.81

Figure 3. Comparison of MRI, MRS and northern blot to quantify *VTC1* and *VMA2* reporter gene expression in yeast. (**A**) Schematic diagram of MRI apparatus. A total of 16 experimental and one reference samples, loaded into 0.8 mm capillary glass tubes, were placed in an 8 mm NMR tube which was then inserted into an NMR spectrometer with an imaging probe. (**B**) The proton density and the polyP-selective images were generated by ^{1}H-MRI (left) and ^{31}P-MRI (right), respectively. The sample number or letter and its position in the grid are shown below the MRI data. 'R' denotes reference and Arabic numerals indicate the promoter construct as described in Figure 1A. 'W' and 'Δ' denote wild type and Δ*vma2* (or Δ*vtc1*) strains, respectively. (**C**) Gene expression was quantified by northern blot (open bar), MRS (grey bar) and MRI (dark grey bar). Results are shown as a percentage of the maximum value in each dataset (asterisk). The values are the average of two (MRI) or three (northern blot, MRS) independent experiments and shown along with the SEM. (**D**) The correlation coefficients between the northern blot and MRS or MRI data were calculated. Data points for gene expression driven by the endogenous *VTC1* or *VMA2* promoters were omitted from the calculations, because they deviated significantly from the exogenous promoters (see text).

V-ATPase, respectively, are suitable as quantitative reporter genes with MRS detection in intact cells. This was done by substituting six heterologous promoters of variable strength (19) for the endogenous promoter region of chromosomal *VTC1* or *VMA2* (Figure 1A). PolyP was then quantified in yeast strains carrying the chromosomal reporter genes with heterologous or endogenous promoters. The results were evaluated to determine if the relationship between the expression of *VTC1* and *VMA2* and the amount of polyP was quantitative.

Yeast cells were cultured to mid-log phase in liquid YPD media and divided into two aliquots. One sample was analyzed by northern blot (Figure 1B and C) and the other was analyzed by ^{31}P-MRS (Figure 1D and E). The northern blot shows very similar expression profiles for *VTC1*, *VMA2* (Figure 1B and C) and the mini-*CLN2* reporter gene characterized previously (19), suggesting that no post-transcriptional regulatory mechanisms influence the steady-state level and/or stability of *VTC1* or *VMA2* mRNA. Furthermore, the amount of mRNA correlates well with the amount of polyP in the vacuole in all

strains with heterologous promoters (Figure 3C #1–6 and D). In contrast, the wild-type (WT) strains accumulate more polyP than expected based on the level *VTC1*/*VMA2* mRNA (Figure 3C). Although the mechanism for this enhanced accumulation is unknown, it is possible that the endogenous *VTC1*/*VMA2* promoters are regulated by an uncharacterized feedback mechanism that leads to increased production of polyP.

In order to provide an accurate measure of gene expression *in vivo*, a reporter system must be temporally responsive; i.e. it must be able to respond quickly to rapid changes in gene expression. This aspect of the polyP system was tested using the inducible *GAL1* promoter to drive gene expression. When the endogenous *VTC1* or *VMA2* promoters are replaced with the *GAL1* promoter, gene expression can be rapidly turned on or off by changing the carbon source in the medium from raffinose to galactose or from galactose to glucose, respectively (20). Kinetic analysis (on-rate kinetics) showed that polyP begins to accumulate (Figure 2A) by 1–2 h after cells are exposed to galactose and induction of *VTC1* mRNA begins (Figure 2C, left). In contrast, the level of polyP does not decrease for at least 24 h after mRNA synthesis is suppressed by changing carbon source (Figure 2B, right); the concentration of polyP remains high, even though *VTC1* mRNA returns to a low basal level within 1 h (Figure 2C, right) and VTC1 protein is also suppressed within 2 h (Figure 2D). One explanation for this result is that may be VTC1 plays a role in initiating vacuolar fusion (21) but does not play a direct role in synthesis of polyP; if this is true, then induction of VTC1 would stimulate accumulation of polyP in the vacuole, but subsequent suppression of VTC1 might not cause a decrease in the level of polyP.

Similar results were observed with *VMA2*, in that the amount of polyP correlated the amount of *VMA2* transcript during induction but not during repression of *VMA2* mRNA synthesis (data not shown). However, the correlation between gene expression and polyP improved when the reporter gene was modified with an N-terminal HA epitope tag. Thus, when an HA-tag was fused to the amino-terminus of VMA2, a decline in *VMA2* mRNA correlated with a decline in polyP, with a lag of a few hours (Figure 2E and F). This more rapid response might indicate that HA-tagged VMA2 has a shorter half-life than VMA2 (data not shown).

The *VTC1* and/or *VMA2* reporter system described above was then tested with MRI detection. The strains shown in Figure 1 were cultured in YPD to mid-log phase and transferred into 0.8 mm glass capillary tubes (Figure 3A) and yeast cultures and a reference sample (i.e. water) were analyzed by MRI (Figure 3B). Signals were integrated longitudinally in each capillary tube and are presented as a bottom view (Figure 3B, right). The average intensity of the polyP image was calculated from ^{31}P-MRI data and the area corresponding to each sample was defined spatially using ^{1}H-MRI data (Figure 3B, left).

Experimental values were measured by northern blot, MRS and MRI, and values were expressed as a percentage of the maximum value for each dataset. The results are summarized in Figure 3C and D. Figure 3D shows the correlation coefficients between northern blot and MRS or MRI methods. These results strongly suggest that gene expression can be quantified accurately by MRS and MRI using *VTC1* or *VMA2* as a reporter gene in yeast cells. To our knowledge, this is the first report describing a fully quantitative reporter system with MRI detection that can be used to monitor spatial and temporal variation in gene expression.

In higher eukaryotes, the endogenous level of polyP is much lower than in yeast (8). In addition, *VTC1* orthologs have not been identified in mammals whereas mutations of *VMA2* orthologs cause genetic disease in humans (22,23). Therefore, in order to apply a similar reporter system in mammalian cells, an exogenous MRI reporter gene may be required. Preliminary results suggest that the *Escherichia coli PPK1* gene, which encodes polyP kinase, is a candidate reporter gene for use in mammalian cells. PPK1 converts the terminal phosphate of ATP to polyP (24), and expression of *PPK1* from a mammalian promoter induced polyP at a level readily detected by MRS or MRI in mammalian cells (unpublished results). Unfortunately, it has not been possible to characterize a *PPK1*-based reporter system in yeast, because the endogenous background of polyP interferes with measurement of induced *PPK1* activity (data not shown). Although organism-specific reporter genes may be needed for future studies in mammalian cells, the system described in this report should be widely applicable.

In summary, this study presents a novel MR-based method for quantifying temporal and spatial variation in gene expression. This method can potentially be used in any tissue of any organism. Furthermore, this method may have important applications in the context of high-throughput cell-based assays, which are used in drug discovery screening and in many other areas of basic and clinical research.

SUPPLEMENTARY DATA

Supplementary data are available at *NAR* online.

ACKNOWLEDGEMENTS

The authors would like to thank members of the Shirakawa and Kokubo laboratories for advice and comments on this work. The authors also thank T. Miyake and M. Longtine for plasmids. This study was supported by grants from the Japan Society for the Promotion of Science, the Ministry of Education, Culture, Sports, Science and Technology of Japan and CREST of Japan Science and Technology Corporation. Funding to pay the Open Access publication charges for this article was provided by the Japan Society for the Promotion of Science.

Conflict of interest statement. None declared.

REFERENCES

1. Tsien,R.Y. (1998) The green fluorescent protein. *Annu. Rev. Biochem*, **67**, 509–544.
2. Contag,C.H. and Bachmann,M.H. (2002) Advances in *in vivo* bioluminescence imaging of gene expression. *Annu. Rev. Biomed. Eng*, **4**, 235–260.
3. Massoud,T.F. and Gambhir,S.S. (2003) Molecular imaging in living subjects: seeing fundamental biological processes in a new light. *Genes. Dev*, **17**, 545–580.

4. Weissleder,R., Moore,A., Mahmood,U., Bhorade,R., Benveniste,H., Chiocca,E.A. and Basilion,J.P. (2000) *In vivo* magnetic resonance imaging of transgene expression. *Nat. Med.*, **6**, 351–355.
5. Louie,A.Y., Huber,M.M., Ahrens,E.T., Rothbacher,U., Moats,R., Jacobs,R.E., Fraser,S.E. and Meade,T.J. (2000) *In vivo* visualization of gene expression using magnetic resonance imaging. *Nat. Biotechnol*, **18**, 321–325.
6. Genove,G., Demarco,U., Xu,H., Goins,W.F. and Ahrens,E.T. (2005) A new transgene reporter for *in vivo* magnetic resonance imaging. *Nat. Med.*, **11**, 450–454.
7. Cohen,B., Dafni,H., Meir,G., Harmelin,A. and Neeman,M. (2005) Ferritin as an endogenous MRI reporter for noninvasive imaging of gene expression in C6 glioma tumors. *Neoplasia*, **7**, 109–117.
8. Kornberg,A., Rao,N.N. and Ault-Riche,D. (1999) Inorganic polyphosphate: a molecule of many functions. *Annu. Rev. Biochem.*, **68**, 89–125.
9. Ogawa,N., DeRisi,J. and Brown,P.O. (2000) New components of a system for phosphate accumulation and polyphosphate metabolism in *Saccharomyces cerevisiae* revealed by genomic expression analysis. *Mol. Biol. Cell.*, **11**, 4309–4321.
10. Wurst,H., Shiba,T. and Kornberg,A. (1995) The gene for a major exopolyphosphatase of *Saccharomyces cerevisiae*. *J. Bacteriol*, **177**, 898–906.
11. Cohen,A., Perzov,N., Nelson,H. and Nelson,N. (1999) A novel family of yeast chaperons involved in the distribution of V-ATPase and other membrane proteins. *J. Biol. Chem.*, **274**, 26885–26893.
12. Lundblack,V. (1998) Saccharomyces cerevisiae. In Ausubel,F.M., Brent,R., Kingston,R.E., Moore,D.D., Seidman,J.G., Smith,J.A. and Struhl,K. (eds), *Current Protocols in Molecular Biology*. John Wiley & Sons, New York, Vol. 2, pp. 13.10.11.–13.13.19.
13. Kitazono,A.A., Tobe,B.T., Kalton,H., Diamant,N. and Kron,S.J. (2002) Marker-fusion PCR for one-step mutagenesis of essential genes in yeast. *Yeast*, **19**, 141–149.
14. Longtine,M.S., McKenzie,A.,3rd, Demarini,D.J., Shah,N.G., Wach,A., Brachat,A., Philippsen,P. and Pringle,J.R. (1998) Additional modules for versatile and economical PCR-based gene deletion and modification in *Saccharomyces cerevisiae*. *Yeast*, **14**, 953–961.
15. Tsukihashi,Y., Miyake,T., Kawaichi,M. and Kokubo,T. (2000) Impaired core promoter recognition caused by novel yeast TAF145 mutations can be restored by creating a canonical TATA element within the promoter region of the TUB2 gene. *Mol. Cell. Biol.*, **20**, 2385–2399.
16. Kotani,T., Miyake,T., Tsukihashi,Y., Hinnebusch,A.G., Nakatani,Y., Kawaichi,M. and Kokubo,T. (1998) Identification of highly conserved amino-terminal segments of dTAFII230 and yTAFII145 that are functionally interchangeable for inhibiting TBP–DNA interactions *in vitro* and in promoting yeast cell growth in vivo. *J. Biol. Chem.*, **273**, 32254–32264.
17. Chen,K. (1999) Study of polyphosphate metabolism in intact cells by 31-P nuclear magnetic resonance spectroscopy. In Schroder,H. and Muller,W. (eds), *Inorganic Polyphosphates.* Springer-Verlag, Berlin, Heidelberg, New York, Vol. 23, pp. 253–273.
18. Hasse,A., Frahm,J., Hanicke,W. and Matthaei,D. (1985) 1H NMR chemical shift selective (CHESS) imaging. *Phys. Ned. Biol.*, **30**, 341–344.
19. Tsukihashi,Y., Kawaichi,M. and Kokubo,T. (2001) Requirement for yeast TAF145 function in transcriptional activation of the RPS5 promoter that depends on both core promoter structure and upstream activating sequences. *J. Biol. Chem.*, **3**, 3.
20. Johnston,M. (1987) A model fungal gene regulatory mechanism: the GAL genes of Saccharomyces cerevisiae. *Microbiol Rev*, **51**, 458–476.
21. Muller,O., Bayer,M.J., Peters,C., Andersen,J.S., Mann,M. and Mayer,A. (2002) The Vtc proteins in vacuole fusion: coupling NSF activity to V(0) *trans*-complex formation. *Embo. J.*, **21**, 259–269.
22. Karet,F.E., Finberg,K.E., Nelson,R.D., Nayir,A., Mocan,H., Sanjad,S.A., Rodriguez-Soriano,J., Santos,F., Cremers,C.W., Di Pietro,A. *et al.* (1999) Mutations in the gene encoding B1 subunit of H+-ATPase cause renal tubular acidosis with sensorineural deafness. *Nat. Genet.*, **21**, 84–90.
23. Smith,A.N., Skaug,J., Choate,K.A., Nayir,A., Bakkaloglu,A., Ozen,S., Hulton,S.A., Sanjad,S.A., Al-Sabban,E.A., Lifton,R.P. *et al.* (2000) Mutations in ATP6N1B, encoding a new kidney vacuolar proton pump 116-kD subunit, cause recessive distal renal tubular acidosis with preserved hearing. *Nat. Genet.*, **26**, 71–75.
24. Akiyama,M., Crooke,E. and Kornberg,A. (1992) The polyphosphate kinase gene of *Escherichia coli*. Isolation and sequence of the *ppk* gene and membrane location of the protein. *J. Biol. Chem.*, **267**, 22556–22561.